Proceedings in MANUFACTURING SYSTEMS

Proceedings in Manufacturing Systems, Volume 21, Issue 2, 2026, pp. 99-109 ISSN 2067-9238

DESIGN AND DEVELOPMENT OF AN AUTONOMOUS MOBILE PLATFORM FOR OPTIMIZING LOGISTICS PROCESSES

Daniela-Mariana ILIE[1], Constantin-Adrian POPESCU[2], Emilia-Maria POPESCU[3], Costel Emil COTET[4,*]

1) PhD Student, National University of Science and Technology POLITEHNICA Bucharest, Romania
2) Lecturer, PhD, Robots and Manufacturing Systems Department, National University of Science and Technology POLITEHNICA Bucharest, Romania
3) Lecturer, PhD, Robots and Manufacturing Systems Department, National University of Science and Technology POLITEHNICA Bucharest, Romania
4) Prof., PhD, Robots and Manufacturing Systems Department, National University of Science and Technology POLITEHNICA Bucharest, Romania

https://doi.org/10.5281/zenodo.22298807

Abstract: *This article presents the design of an AMR (autonomous mobile robot), as well as the main equipment and components required for its construction and operation. The robotic platform developed is intended for product transport and handling applications within logistics and warehousing processes. In this context, the article presents the solutions adopted for the mechanical structure, the locomotion system, and the lifting mechanism, as well as the method for integrating the electrical and electronic components. The article also highlights the sensor system used to acquire the information necessary for the robot's operation and the control architecture based on ROS 2. The main structural and functional elements of the platform are described, as well as the method of interconnection and communication between them. Experimental evaluation across six scenarios indicates an average reduction in energy consumption of 18.0% and in duration of 12.5%, while the success rate increased from 87.3% to 96.5% compared to classical A* planning.*

Keywords: *AMR (autonomous mobile robots), energy planning,* automation, logistics flow, *distribution warehouse, ROS 2, SLAM.*

1. INTRODUCTION

The autonomous mobile robot (AMR) has become a practical solution for internal transportation in factories and warehouses, as it can change its route without physically reconfiguring the infrastructure. Unlike an automated guided vehicle, which relies on a lane, reflectors, or a fixed sequence of waypoints, an AMR estimates its current position, interprets the available space, and adjusts its motion control accordingly. The resulting flexibility is important in areas where pallets, carts, and operators frequently alter the navigable geometry [6, 7].

In a rack-handling application, range cannot be analyzed separately from the platform's mechanics. The robot must move under the structure being transported, adjust its position without a wide maneuver, lift the load, and leave the area with a sufficient safety margin. Any play in the vertical guides, frame deformation, or slippage of the Mecanum wheels affects odometry. At the same time, an improper LiDAR sensor position can mask low obstacles or cause the laser scan to intersect with the robot's components.

The platform under review uses a modular frame made of aluminum profiles, four independently driven Mecanum wheels, a central screw-type lifting mechanism, and four linear guides. A 2D RPLIDAR A1M8 LiDAR provides the primary environmental perception, while encoders, the inertial unit, and near-field sensors complement the state estimation. The configuration allows for longitudinal translation, lateral translation, diagonal movement, and rotation around the geometric center. These modes are used as primitives from which approach and docking trajectories are composed.

The objective of this article is to provide an integrated evaluation of the three levels that determine motion: mechanical structure, LiDAR perception geometry, and trajectory generation. The contribution lies not in a new overview of the robot, but in explaining the interfaces between these levels. The study examines the position and rigidity of the LiDAR mount, the propagation of geometric uncertainty into the local map, the influence of the scanning frequency on obstacle avoidance, and the use of holonomic mobility for short lateral corrections.

The structure of this paper follows the format of an experimental article. Section 2 summarizes current approaches relevant to mechanics, perception, and planning. Section 3 describes the platform, the kinematic model, the LiDAR setup, and the evaluation metrics. Section 4 defines the scenarios and the experimental procedure. Section 5 discusses the calculated results and design implications, and Section 6 presents the conclusions and limitations of the study.

* Autor de corespondență: Splaiul Independenței 313, Sector 6, 060042, Bucharest, Romania,
Telefon: 0040 402 9420,
Adrese de e-mail: *daniela_ilie96@yahoo.com* (D.-M. Ilie)

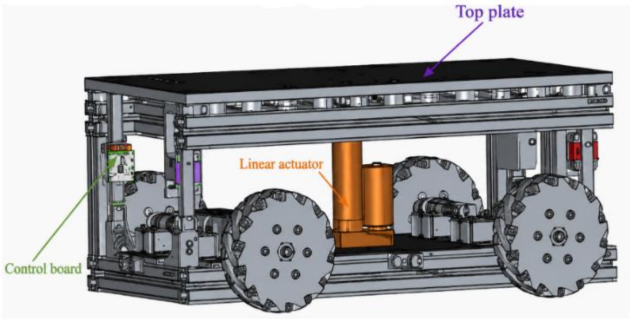

Fig. 1. General Structure of the AMR

The application – subject of this work – involves the handling of mobile shelves: the platform is positioned under a loaded shelf, lifts the structure a limited distance (50 mm) to lift the shelf off the ground and transports it to the picking, sorting or storage areas (Fig. 1).

2. THE CURRENT STATE OF AUTONOMOUS MOBILE ROBOTS

Intralogistics automation has evolved from automated guided vehicles – which rely on lanes, markings, or dedicated infrastructure – to autonomous mobile robots capable of locating themselves, planning their routes, and responding to changes. This transition is not merely a matter of terminology. An AGV typically follows a predetermined route and treats deviations as exceptions, while an AMR continuously recalibrates the relationship between its position, the map, obstacles, and the logistics objective. In the intralogistics literature, the advantage of AMRs is associated with flow flexibility, rapid reconfiguration, and integration into production systems with high variability.

An analysis of mobile robotic systems designed to perform tasks shows that performance does not depend solely on the vehicle's speed. Task allocation, the location of inventory, loading points, and cooperation with the operator can substantially alter the duration and energy consumption of a mission. For this article, this observation has a direct methodological implication: the navigation algorithm must be evaluated for a complete mission, not just for the geometric length of the route. A short route can result in more stops, turns, and restarts, and the total energy consumption can become much higher.

In an industrial setting, the benefit of an AMR depends on its availability and repeatability. A configuration that saves energy on average but results in frequent recoveries or malfunctions that are difficult to diagnose is not superior from an operational standpoint. For this reason, the current state is analyzed simultaneously from the perspectives of navigation, energy, robustness, and traceability. These four dimensions will subsequently become common criteria for evaluating original contributions..

Recent research also highlights a shift in the unit of optimization. In classical systems, each vehicle can be analyzed separately. In a flexible cell, the robot's mission interacts with loading processes, stations, and other resources. Even though this thesis focuses on a single robot, the data structure and metrics are defined so that the results can later be scaled up to the fleet level, without confusing local optimization with the performance of the entire system.

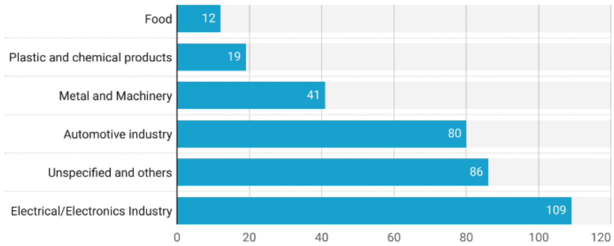

Fig. 2. The main industries in which AMRs are used.

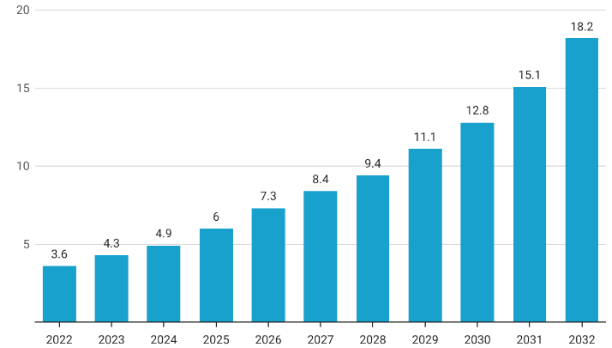

Fig. 3. Significant increase in the market presence of AMRs.

2.1. Statistics on the use of autonomous mobile robots in logistics applications

Autonomous mobile robots (AMRs) locate their position, interpret their environment, and replan their path without physical guides. In intralogistics, they are used for transport, line feeding, picking, and sorting, as they can be integrated into workflows that change more frequently than fixed infrastructure.

The market data summarized in Figs. 2 and 3 confirm the rapid expansion of AMRs and their concentration in warehouses and distribution centers. The increase in the number of installations is shifting the focus from simple autonomous movement to integration with order management, battery availability, and mission performance metrics.

Autonomous mobile robots (AMRs) have seen significant growth in recent years and are used in a variety of economic sectors where transportation, handling, supply, and autonomous movement can be automated.Beneficiile şi impactul AMR-urilor în cadrul unui flux:

- Efficiency and Productivity – The implementation of mobile robots has led to an increase in operational efficiency of up to (30 to 40)%, and order processing time has been significantly reduced, while inventory management accuracy has also improved significantly.
- Operating costs – Although the initial cost of implementing mobile robots can be significant, in the long term, operating costs are reduced due to the automation of repetitive tasks and the reduced need for human labor

Statistical analysis indicates that the growth of AMRs should not be interpreted solely in terms of the increase in the number of robots sold, but rather in terms of the changing structure of the logistics flows into which they are integrated. Increased adoption is driving a transition from using AMRs for one-off internal transport operations to integrating them into successive activities such as picking, replenishment, sorting, and shipping. Looking ahead to 2032, the main anticipated change lies not only in the increase in the number of robots but also in the greater degree to which they are integrated into the warehouse's information and operational systems.

Furthermore, statistical data indicate that transportation and logistics currently constitute the primary sector for the use of mobile robots, and the development of this field is closely linked to the automation of warehouses, distribution centers, and internal material flows. The high proportion of logistics applications justifies focusing research on the integration of AMRs into warehouse processes and, in particular, on their use to streamline order-picking activities.

3. STRUCTURE AND CONFIGURATION OF THE AUTONOMOUS MOBILE ROBOT

For an industrial distribution warehouse, shelfpicking AMR must meet at least the following
requirements:

- Holonomic mobility for precise alignment with the rack and maneuvering in tight spaces (aisles, loading areas).
- Controlled vertical lifting, with mechanical self-locking in the event of a power outage.
- Estimating motion state (velocity, position, orientation) by combining odometry with inertial measurements.
- 2D environmental perception for mapping, localization, and obstacle avoidance; additional near-field detection for low-reflectivity or non-reflective objects.
- Monitoring the load (presence, mass, distribution) for safety and to adjust dynamic behavior.
- Modular architecture for maintenance (quick replacement of a motor, sensor, or power module) and for rapid design iterations (Fig. 4).
- Safety features: emergency stop, speed limitation when people are nearby, collision detection, and power supply protection.

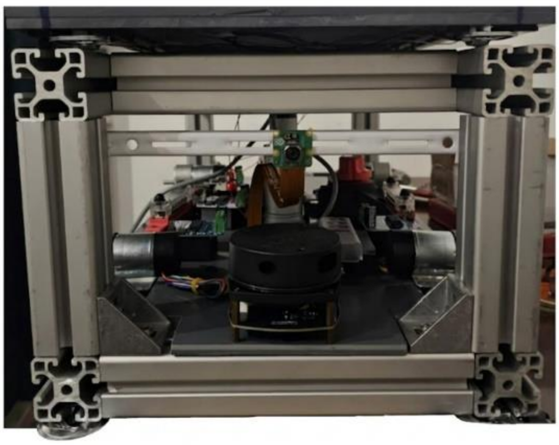

Fig. 4. The AMR's modular chassis.

3.1. Mechanical architecture of the platform

Modular frame made of 40 × 40 mm aluminum profiles (8-channel). The load-bearing structure is made of 40 mm × 40 mm extruded aluminum T-profile (channel 8) sections, assembled with 40 mm × 40 mm × 25 mm aluminum angle brackets and screws. The choice of this type of frame has direct implications for rigidity, weight, ease of maintenance, and the ability to reconfigure the structure.

PVC mounting plates: lower platform and movable upper platform. A rigid PVC plate (6 mm thick) is mounted on the lower frame and serves as a base for the electronic components and some of the sensors. The movable upper frame uses a 12 mm PVC plate, which functions as a mechanical interface with the shelf and as a mount for the weight sensors. Both plates are secured with screws, allowing for quick disassembly and access to the subassemblies.

Considerations Regarding the Use of PVC in Mobile Structures:

PVC is lightweight, has relatively good internal damping, and is easy to machine (drilling, cutting), making it suitable for prototyping.

Bending stiffness is lower than that of metals; to limit deformation under load, it is important to provide contour support and, if necessary, stiffening ribs or to replace the material with composite or aluminum panels.

Temperature and creep behavior must be taken into account: under a constant load, deformations may increase over time, especially at high ambient temperatures or when electronic components are hot.

Holonomic drive system: Mecanum wheels and DC motor drives with encoders. The platform's mobility is provided by four Mecanum wheels (with a diameter of ~120 mm), each driven independently by a DC motor with a gear reducer (30:1 ratio) and a quadrature incremental encoder. Mecanum wheels are characterized by inclined rollers (typically at 45 °), which allow for the generation of force components in both the longitudinal and lateral directions of the chassis. By combining the angular velocities of the four wheels, the vehicle can perform translational movements along the X and Y axes and rotation around the Z axis without changing its orientation (holonomic motion).

From a structural standpoint, the motors are mounted using L-shaped brackets (cantilever) and dedicated wheel mounts. This design facilitates maintenance, as it allows for the replacement of a motor or wheel without having to disassemble the chassis. However, for industrial operation, it is important to check the alignment of the shafts and to reinforce the brackets to prevent elastic deformation under torque (which can cause contact variations and vibrations).

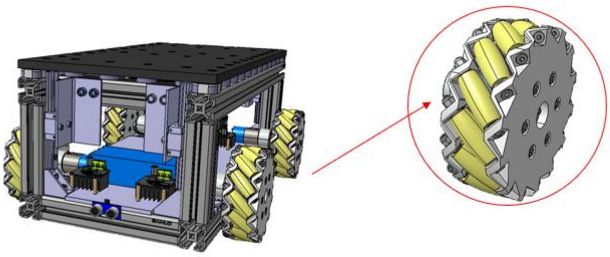

Fig. 5. AMR Wheel.

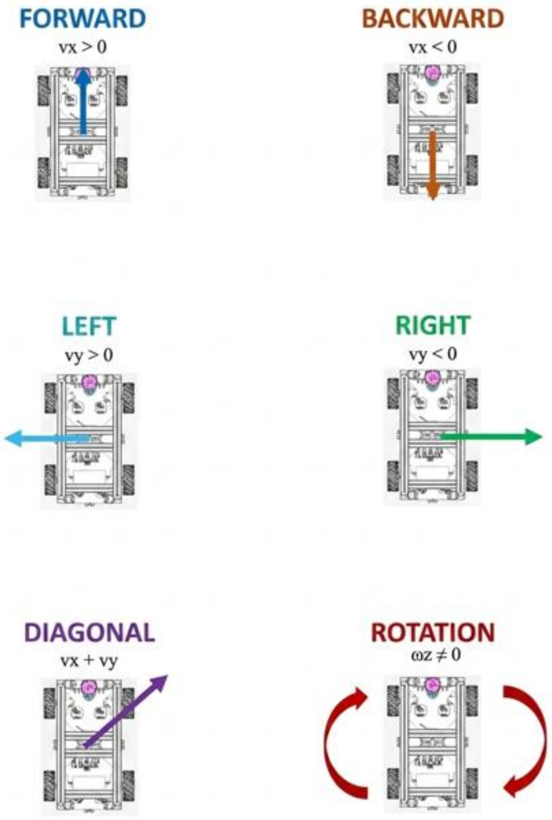

Fig. 6. Mecanum base motion primitives for translation and alignment.

Lifting module: irreversible electric linear actuator (screw type) and movable upper frame. The shelf is raised by a lifting mechanism featuring an electric linear screw-and-nut actuator (irreversible, self-locking configuration), mounted centrally between the lower (fixed) and upper (movable) frames. The selected actuator, model LD3-24-20-K3, is powered by 24 VDC and provides a thrust/pull force of approximately 500 N, a nominal speed of about 12.3 mm/s, and a stroke set to 50 mm. The stroke meets the requirement to lift the shelf by approximately 5 cm, which is sufficient to clear the floor and overcome minor floor irregularities.

The advantages of choosing a screw-type (non-reversible) actuator for lifting are teh folowing (Fig. 7):

- Mechanical self-locking: In the event of a power outage, the screw mechanism tends not to be driven in the opposite direction of the load, maintaining the height without consuming energy.
- Easy position control: displacement is proportional to the number of rotations; combined with a feedback system (Hall sensor/encoder), this enables closed-loop control of the stroke.

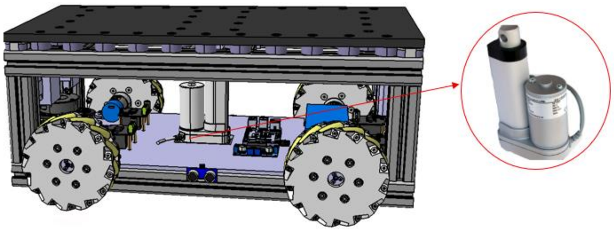

Fig. 7. AMR Lifting Module.

Fig. 8. Linear Guides.

- High force capacity in a compact design, without the need for a pneumatic or hydraulic system.
- Easy integration into the modular system: the actuator can be replaced as a single unit, and the fasteners can remain standardized.

Z-axis guidance: TRH15/TRS15 (TBI Motion) linear guides in a four-corner configuration. To ensure a strictly vertical lifting motion, without oscillations and without lateral loads on the actuator, the movable upper frame is guided by four guide assemblies mounted at the corners. Each assembly consists of a profiled rail (TR 15 series) and a carriage (TRS15 series) with recirculating balls, which ensures a low coefficient of friction and high rigidity under combined loads. The 15 mm guides are designed for dynamic loads of up to ~11.8 kN and static loads of up to ~21.6 kN per block, with allowable moments in the range of ~100 Nm to 160 Nm, depending on the block type (flanged/standard) (Fig. 8).

Some advantages of using linear guides can be listed:

- Separating the function of support and guidance from that of actuator: The actuator applies force in the Z direction, while the guides absorb the lateral moments and forces induced by the load and the platform's acceleration.
- Control of play and parallelism: By using preloaded carriages (with play/standard/light), play can be reduced, improving docking repeatability and load stability.
- High torsional stiffness: The placement of the guides in the corners increases the leverage effect between them, enhancing the ability to absorb the torques generated by an unevenly loaded shelf.
- Industrial-grade durability: recirculating ball guides are designed for a high number of cycles and can be lubricated periodically; seals reduce dust contamination.

Load monitoring: load cells and elastic decoupling with rubber pads. The movable top plate (12 mm PVC) incorporates a weight sensor (load cell, max. 50 kg) in each corner. Rubber pads are inserted between the upper frame and the plate, and the assembly is secured with screws. This design allows for controlled mechanical contact between the load (shelf) and the sensing elements, as well as damping of vibrations transmitted from the chassis to the load (Fig. 9).

The functional roles of weight sensors are as follows:

- Lift detection: A sudden increase in the measured force indicates that the shelf has been lifted and the weight has been transferred to the platform.

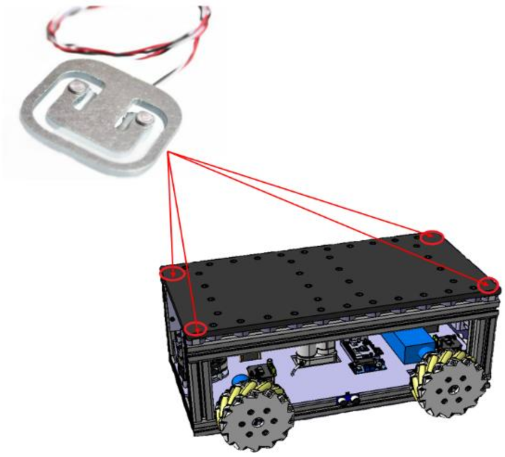

Fig. 9. AMR Load Monitoring.

Fig. 10. Assembly and wiring components.

Fig. 11. AMR Battery.

- Estimating the load mass: the sum of the four cells allows you to estimate the total mass and verify that the load is within the permitted limits.
- Estimating the center of gravity (CoG) in the plane: the distribution across the four corners can be used to estimate the eccentricity of the load and to adjust speed and acceleration.
- Anomaly detection: Unexpected variations (for example, a drop at a corner) may indicate that the shelf is slipping, uneven contact, or a mechanical malfunction.

Among the functions of rubber pads (elastic decoupling) we can mention:The role of rubber buffers (elastic decoupling):

- Damping of high-frequency vibrations generated by the Mecanum wheels, improving load stability and the quality of the signal from the load cells.
- Reduces shock peaks upon initial contact with the shelf, protecting both the frame and the sensors.
- Compensating for minor geometric imperfections (flatness) and ensuring a more uniform distribution of force.

Assembly and maintenance components: angle brackets, screws, spacers, and cable management

The assembly is primarily put together using threaded fasteners (screws) and standardized parts: angle brackets, spacers, clamps, heat-shrink tubing, and modular connectors. In an industrial setting, this choice has a direct impact on ease of maintenance and reliability.

Among the advantages, the following can be highlighted:

- Quick disassembly and replacement of subassemblies, without irreversible operations (welding, structural bonding).
- Traceability of maintenance: Components can be replaced individually, and torque settings can be checked periodically.
- Easy integration of the cable management system and physical separation between power and signal (spacers, channels, clamps) (Fig. 10).

3.2. Electrical and electronic architecture

Power supply: 6S2P Li-ion battery, 24 V output, and DC-DC converters. The system is powered by a 6S2P Li-ion battery with a nominal capacity of 10 Ah (10,000 mAh). A 6S battery has a nominal voltage of approximately 22.2 V (3.7 V/cell) and a maximum charging voltage of 25.2 V (4.2 V/cell), making it compatible with architectures generically referred to as “24 V.” The stored energy is on the order of 22.2 V × 10 Ah = 222 Wh, a useful value for estimating runtime. To power the onboard computer and low-voltage sensors, DC-DC step-down converters are used to step down the voltage from 24 V to 5 V, with an output current in the range of amperes (Fig. 11).

Drive systems and power electronics: DC motors with gearboxes, encoders, and H-bridge drivers. Each Mecanum wheel is driven by a DC motor with a 30:1 metal gear reducer and a quadrature incremental encoder. An example of such a motor (Pololu 37Dx68L 24 V, 30:1) offers a no-load speed of approximately 330 rpm and a holding current of about 3 A, with a maximum torque of ~15 kg*cm (approx. 1.47 N*m). The integrated encoder provides 64 pulses per revolution (CPR) at the motor shaft, equivalent to ~1.920 CPR at the output shaft after the gearbox, which allows for accurate estimation of wheel speed and odometer reading.

Bidirectional motor control is achieved using H-bridge drivers (BTS7960). These modules integrate power MOSFETs and protection circuits (overcurrent, overheating, undervoltage), making them suitable for 24 V DC drives with “ ”-type current spikes at startup. Control is achieved via logic signals (PWM and direction), and in applications with high dynamic requirements, it is recommended to implement encoder-based closed-loop speed control (PID).

Tire Pressure Monitoring. The bill of materials (BOM) includes an INA219 (I2C) current sensor, which can be used to measure the current drawn by subassemblies. By measuring the motor current, diagnostic functions can be implemented: detection of wheel lockup, collisions, or slippage when the current increases without a corresponding increase in speed or odometer reading. In addition, the average current can be used to estimate energy consumption and remaining range.

The electrical architecture separates the motors’ power bus from the logic branch. The battery powers the drive stages and the DC/DC converter, the microcontroller generates the PWM signals, and the Raspberry Pi runs the ROS 2 functions for localization, planning, and supervision. The emergency stop cuts off power to the motors via a path independent of the software, while the logic branch can retain the logs necessary for diagnostics. For energy balance, U(t) and I(t) are acquired synchronously from the main battery; measuring a single branch remains useful only for local diagnostics.

3.3. Sensors for navigation, safety, and interaction

LIDAR 2D for mapping and positioning. The main sensor for environmental perception is a 2D LIDAR of the RPLidar A1M8 type, capable of 360 ° scanning in the horizontal plane, with a typical range of up to 12 m under favorable conditions. The physical mounting and the relationship between the laser frame and the base frame are shown below in Figs. 12 and 13.

The sensor generates a 2D point cloud (a set of distances as a function of angle) with a typical scanning frequency of 5.5 Hz and can be configured up to approximately 10 Hz, with a sampling rate of (4 to 8) kHz. This type of sensor is suitable for 2D SLAM (Simultaneous Localization and Mapping) algorithms, enabling the construction of a warehouse map and the localization of the robot by correlating current scans with the map.

Several advantages can be listedAdvantages:

- Independence from external markers: the robot can navigate based on the geometry of its environment (walls, shelves) without physical guides.
- Sufficient accuracy for navigation and obstacle avoidance in indoor environments, particularly in hallways with repetitive layouts.
- Mature software integration: There are established drivers and navigation stacks (e.g., ROS/ROS2) for this type of LIDAR.

Near-field proximity sensors: ultrasonic and ToF. To cover the near field and detect obstacles at short distances, the system uses HC-SR04 ultrasonic sensors (mounted on the sides and rear) and a laser-based Time of-Flight (ToF) sensor (model VL53L1X). The ultrasonic sensors are resistant to ambient light and can detect objects with various textures, while the ToF sensor provides good resolution at short distances and can detect edges or slopes in the immediate vicinity of the chassis (for example, to prevent falling off a ramp or platform).

Inertial Sensors and Visual Perception. To estimate orientation (particularly yaw) and improve odometry, the platform includes an IMU (9-axis: gyroscope, accelerometer, magnetometer, MPU-9250 type). IMU data allow for the compensation of odometry errors caused by slippage, and filtering (e.g., the extended Kalman filter) can ensure a robust state estimate.

The bill of materials (BOM) includes a Raspberry Pi camera (Camera Module 3), designed for visualization functions: shelf identification (QR codes/AprilTags), work area monitoring, and potential artificial intelligence functions (object/person detection). In industrial practice, vision can enhance the robustness of docking by complementing LIDAR in situations involving geometric symmetry (identical colors) or in crowded areas.

Control unit: Raspberry Pi as the upper level and a microcontroller as the lower level. The control architecture is built around a Raspberry Pi 5 onboard computer (8 GB RAM) running the operating system (Linux) and high-level software components: communications, perception, SLAM, planning, and supervision. Persistent storage for the system and code is provided via a microSD card. For real-time functions (reading the high-frequency encoder, deterministic PWM generation, rapid safety monitoring), the bill of materials (BOM) includes a microcontroller (Raspberry Pi Pico 2 W), which can act as a lower-level control subsystem.

There are a few reasons for separating the Pi from the microcontroller:

- The Raspberry Pi is not a strictly real-time system; latencies may vary due to the process scheduler. The microcontroller can run PID loops at hundreds of Hz to kHz with deterministic latency.
- Quadrature encoders require precise counting; the microcontroller can use dedicated peripherals (PIO/interrupt) and send only the filtered speed/position to the Pi.
- Safety channels: The microcontroller can shut down the motor drivers upon detection of a critical event (overcurrent, emergency stop signal), independently of the higher-level software.
- Scalable architecture: Additional functions (e.g., controlling the lift actuator, reading the HX711 sensor) can be assigned to the microcontroller without overloading the Pi. Communication between layers can be achieved via UART, USB, or I2C, using a simple protocol (e.g., messages with CRC) or by integrating ROS2 via micro-ROS. The choice depends on the acceptable latency and the complexity of the system.

3.4. Software architecture and features

For a research platform dedicated to autonomous navigation in warehouses, a recommended approach is to use standardized robotics middleware (e.g., ROS2), which facilitates modularization into “nodes” (processes) and message exchange between components. The Raspberry Pi 5 can run ROS2 on a compatible Linux distribution, and typical nodes include: sensor drivers (LIDAR, IMU, camera), odometry, sensor fusion, SLAM/localization, path planning, speed control, and monitoring. The microcontroller can run dedicated firmware for motor control and can publish/consume messages via a serial interface.

Mecanum wheel kinematics and speed control. For a classic Mecanum configuration (wheels at 45 °), the relationship between the wheel speeds and the platform speed can be expressed as a matrix. Let r be the wheel radius, Lx and Ly the distances between the center of the platform and the wheel’s contact point along the X and Y axes, respectively, and $w1...w4$ the angular velocities of the wheels. A common form (for a specific numbering convention) is:

$$vx = (r / 4) \cdot (w1 + w2 + w3 + w4), \quad (1)$$

$$vy = (r / 4) \cdot (-w1 + w2 + w3 - \mathrm{w4})\mathrm{wz} = (r / (4 \cdot (Lx + Ly))) \cdot (-w1 + w2 - w3 + w4), \quad (2)$$

where vx and vy are the linear velocities in the plane, and wz is the angular velocity about the vertical axis. In practice, these relationships are used in two ways: (i) to calculate wheel commands based on platform commands (inverse kinematics) and (ii) to estimate platform motion based on data from encoders (direct kinematics).

It is recommended that wheel speed control be of the closed-loop (PID) type based on encoders, with acceleration limits to reduce slippage. Since the Mecanum wheel has cross-axial coupling and is sensitive to differences in friction between the wheels, careful calibration of the PID constants and conversion factors (pulses to rad/s) is essential. Additionally, implementing feedforward control (voltage proportional to the desired speed) can reduce steady-state error.

State estimation (odometry + IMU): sensor fusion. Mecanum odometry, derived from encoders, is affected by slippage and vibrations. Therefore, it is recommended to fuse it with IMU data in an estimation filter (e.g., the extended Kalman filter – EKF). In a ROS2 implementation, a common package is “robot_localization,” which can combine angular velocity measurements and gyroscope accelerations with wheel odometry. The result is a more robust estimate of position (x, y) and orientation (yaw), which can be used as input for map-based localization (AMCL) or SLAM.

SLAM 2D and warehouse navigation. The LiDAR sensor was integrated into the mechanical structure of the robotic platform to ensure the best possible visibility of the surrounding area. Its position was determined based on the chassis geometry, the platform’s height, and the positioning of the other mechanical components.

The LiDAR is mounted on a rigid bracket attached to the robot's frame, a solution that ensures the sensor remains in position during movement. The bracket's placement allows scanning to be performed without the detection field being significantly obstructed by chassis components or the lifting mechanism.

From a design perspective, the LiDAR mount is integrated into the robot’s mechanical assembly, providing both protection for the sensor and access to it for inspection or maintenance. The sensor’s central and rigid positioning helps ensure stable measurements, which are then used for the platform’s autonomous localization and navigation.

Based on 2D LIDAR data, the platform can run a 2D SLAM algorithm to build a grid-based map of the warehouse’s spatial layout. In structured environments (rows, shelves), algorithms such as GMapping, Hector SLAM, or Cartographer 2D can be used, each with specific advantages: Hector SLAM can perform well without precise odometry at low speeds, while Cartographer uses global-local optimization and can provide better consistency in closed loops. Once the map is built, localization can be performed using AMCL (Adaptive Monte Carlo Localization) by matching scans.

Motion planning in ROS2 is typically carried out using a global planning component (e.g., A* or Dijkstra on a map) and a local control component (e.g., DWB, TEB) that generates velocity commands while adhering to dynamic constraints and avoiding obstacles detected in real time. Proximity information (ultrasonic, ToF) can be integrated as additional layers into the “cost map” to improve safety in the near field.

Figure 12 shows the actual mounting of the sensor on the platform, and Fig. 13 illustrates its position in top and side views. The extrinsic transformation between the laser frame and the base frame is incorporated into the kinematic model so that the measured points are correctly projected onto the robot’s map. The 2D LiDAR sensor measures the distance and angle relative to surrounding surfaces. The resulting point cloud identifies walls, shelves, and obstacles and serves as the primary input SLAM, localization, and cost map updating (Fig. 14).

The AMR platform’s movement path is determined based on the configuration of the workspace and the position of obstacles identified by the LiDAR sensor. In warehouses organized into aisles and picking zones, the robot must be able to move forward, backward, and sideways, as well as change direction, while maintaining a safe distance from shelves and other obstacles.

Thanks to its four-wheel Mecanum configuration, the platform can move not only forward and backward but also sideways and rotate around the vertical axis. This feature allows the robot to navigate tight spaces in the warehouse and facilitates its positioning at load pickup and drop-off areas.

S0 – Target search: identifying the shelf using a map, visual markers, or predefined coordinates. S1 – Approach: overall planning to navigate to the vicinity of the shelf at a reduced speed.

S2 – Fine alignment: use of lateral movement (Mecanum) and proximity sensors to center under the shelf. S3 – Position confirmation: verification via LIDAR/ToF/ultrasound and, if necessary, a camera; optionally, verification of the absence of obstacles.

S4 – Lifting: actuator control at 50 mm, monitoring of actuator current and signals from the load cells.

S5 – Load verification: confirmation of weight transfer (increase in load cell readings) and validation of distribution; if distribution is uneven, alignment may be repeated.

S6 – Transport: flight with a speed profile adapted to the mass and center of gravity (CoG). S7 – Landing: controlled descent, confirmation of separation, retraction.

The sequence for docking and lifting the rack. Manipulating the shelf requires a controlled sequence, which can be implemented as a finite-state machine (FSM):

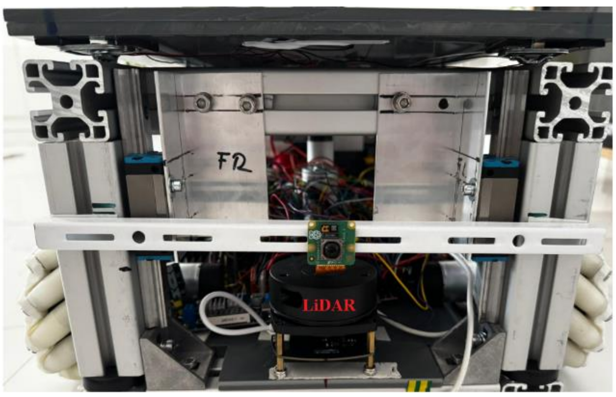

Fig. 12. The AMR's LiDAR sensor.

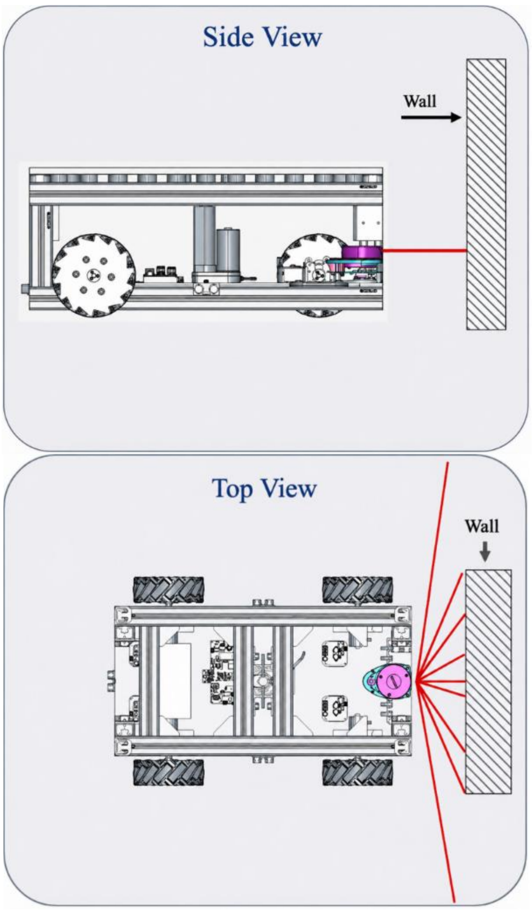

Fig. 13. Top and side views for LiDAR mounting and frame transformation.

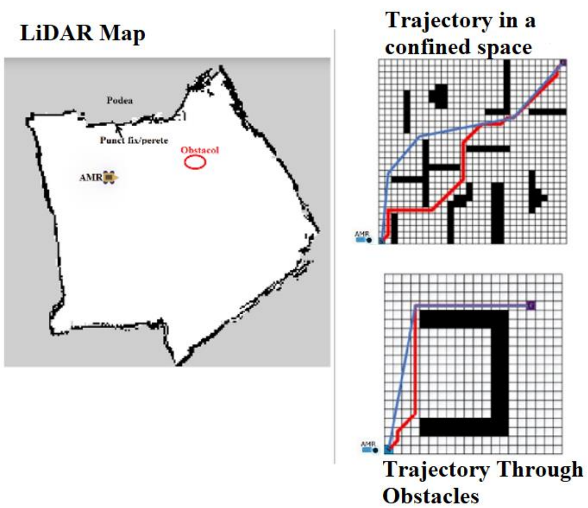

Fig. 14. SLAM and AMR Odometry: LiDAR Map and Trajectory Examples.

S0 – Target search: identifying the shelf using a map, visual markers, or predefined coordinates. S1 – Approach: overall planning to navigate to the vicinity of the shelf at a reduced speed.

S2 – Fine alignment: use of lateral movement (Mecanum) and proximity sensors to center under the shelf. S3 – Position confirmation: verification via LIDAR/ToF/ultrasound and, if necessary, a camera; optionally, verification of the absence of obstacles.

S4 – Lifting: actuator control at 50 mm, monitoring of actuator current and signals from the load cells.

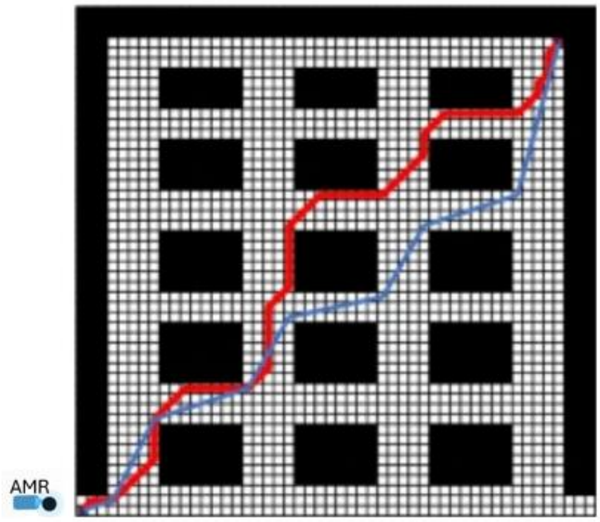

Fig. 15. The routes taken by the AMR within the warehouse.

S5 – Load verification: confirmation of weight transfer (increase in load cell readings) and validation of distribution; if distribution is uneven, alignment may be repeated.

S6 – Transport: flight with a speed profile adapted to the mass and center of gravity (CoG). S7 – Landing: controlled descent, confirmation of separation, retraction.

In practice, the lifting process must include safety logic: stopping when a current threshold is exceeded (indicating a jam), stopping when the end of the stroke is reached, and limiting the lifting speed to prevent over-excitation. Load cells allow detection of the moment when the shelf actually "lifts" (before the end of the stroke), precise control.

3.5. Considerations regarding use in actual industrial warehouses

Interaction with the environment: flooring, color, reflectivity. Industrial warehouses exhibit significant variability: concrete surfaces with joints, dusty areas, glossy surfaces or markings, variations in lighting, as well as dynamic obstacles (operators, forklifts, pallets). Mecanum wheels perform best on flat, clean surfaces; to increase robustness, the following is recommended:

- selecting rollers made of a material that is wear-resistant and provides good adhesion to the finished concrete;
- limiting speeds and acceleration in areas with joints or slopes;
- mechanical protection of the rollers and periodic cleaning;
- defining operating corridors with adequate flatness (where possible).

Operational Safety. In an industrial setting, safety is essential. The prototype described includes an emergency stop switch and obstacle detection channels, but to comply with the specific standards for unmanned industrial vehicles, additional measures are required: certified safety sensors (e.g., safety lidar or safety zones), redundant architectures, risk assessment (FMEA/FTA),

Table 1

Main and auxiliary components used in the prototype

No.	Compound	Quantity	Role
1	Raspberry Pi 5 Model B cu 8 GB RAM	1	Development board (embedded computer)
2	64 GB microSD card	1	Storage space for the operating system and source code
3	Raspberry Pico 2W	1	Battery Protection and Balancing
4	24 V Li-ion batteries	1	Wireless Power Supply
5	Convertor CC-CC 24 V -> 5 V	2	Powering the Sensors and the Raspberry Pi with a Battery
6	Motor Drivers	4	For engine control
7	Roti-motion Power Switch	2	Safety
8	Set of 120 mm Mecanum/Omni Wheels	2	Movement
9	24 V motor, 30:1 gear ratio, with encoder	4	Movement
10	6 mm PVC sheet, 1000 x 2000 mm	1	Mount for electronic components and certain sensors
11	RPLidar	1	Mapping sensor
12	HC-SR04 Ultrasonic Sensor	4	Distance Sensor
13	IMU Sensor	1	For reference
14	Pi 3 Camera Module	1	AI Vision
15	PIR Sensor	3	Motion detection, human presence
16	Weight Sensors	4	Load weight
17	Wheel current sensors	1	Detection of Locked or Skidding Wheels

and fail-safe behaviors. PIR sensors, standard ultrasonic sensors, and uncertified lidar systems can aid in detection, but they are not typically accepted as standalone safety elements (Table 1).

Based on the CAD renderings and the description provided, the concept is functional in principle: the platform features holonomic mobility for alignment, a lifting mechanism with adequate stroke (50 mm), and vertical guidance capable of stabilizing the upper frame. The sensor architecture (2D LIDAR + proximity sensors + IMU) is sufficient for a prototype of autonomous indoor navigation, and the use of load cells adds a valuable channel for confirming shelf pickups and diagnostics.

4. THE EXPERIMENTAL PART OF AMR

The experimental part verifies whether the mechanisms presented produce the anticipated effect at the mission level. The unit of analysis is a complete transition from a controlled initial state to a defined target. Energy, time, distance, and events are integrated into the same time window. Failures are retained and classified; they are not removed from the dataset.

Before a series of operations, the pressure and play of the rollers, the load securing, the battery voltage, the sensors, and the emergency stop (E-STOP) response are checked. The mobile platform is returned to the same starting position, and its location is initialized using the same procedure. The active map and the manifest are recorded in the log.

The floor is cleaned and inspected. For the low-friction scenario, the material and surface are defined in a controlled manner and do not extend beyond the marked area. Temporary obstacles are marked with physical markers. The corridors are measured so that the footprint remains feasible for all methods.

The battery is brought to a defined state of charge. The test cycles do not combine the start of a fully charged battery with the end of an uncontrolled or covariate deep discharge. Ambient and engine temperatures are recorded when the instruments allow it.

The power analyzer is checked at zero and under a known load. Its clock is synchronized with ROS 2 events. A brief test command confirms the power polarity and the presence of startup spikes before the first mission.

In S5, the low-adhesion zone is positioned so that the geometric trajectory crosses it and the alternative route is feasible. The first run may enter the zone and generate memory. Subsequent runs verify the effect of the replanning. In S4 and S8, the temporary obstacle does not overlap with the wall; it blocks part of the corridor and allows for separate observation of the active layer.

The evaluation is organized into four tests that progressively isolate sources of error (Table 2). T1 checks the sensor and the mount with the robot stationary. T2 adds movement along a straight path and examines the influence of mechanics on odometry and scanning. T3 introduces a temporary obstacle and verifies the transition from global trajectory to local correction. T4 evaluates approach and alignment under a shelf using the lateral component of the Mecanum base.

Table 2

Scenarios and Evaluation Indicators

Test	Condition	Key Indicator
T1	wall-mounted	distance dispersion, valid radii
T2	longitudinal movement along the aisle	transverse error, dmin
T3	an obstacle placed along the route	latency, deviation, shutdown
T4	approach and side docking	*x*/*y* offset and final angle

The environment is measured before the test. The width of the corridor, the position of the reference wall, and the dimensions of the obstacle are recorded in a sketch. The static map remains unchanged throughout the test series. The temporary obstacle is not included in the map and is placed only after the location has been initialized. Thus, the observed reaction stems from the current scan, not from prior knowledge of the geometry.

5. RESULTS

The experimental evaluation used six representative scenarios (Fig. 16): open corridor (S1), dense sequence of turns (S2), driving near a wall (S3), dynamic obstacle (S4), low-traction area (S5), and cargo transport followed by docking (S6). For each run, the energy drawn from the battery, distance, duration, replanning events, and mission outcome were synchronized. The initial conditions, state-of-charge range, and obstacle positions were kept constant across methods.

The reduction in energy consumption ranges from 9.7% in S1 to 22.4% in S4. The vales of 19.9% in S5 and 18.3% in S6 confirm the advantage under low-traction and loaded conditions.This effect results from a reduction in stops and reversals.

The average duration decreases from 40.8 s to 35.7 s, and the success rate increases from 87.3% to 96.5%. The distance remains nearly unchanged (13.68 m versus 13.72 m), so the improvement stems from a smoother execution, not from shorter missions.

Compared to Theta* + DWA and A* + DWA (Fig. 17), the proposed method combines minimum runtime with maximum success. Energy consumption, the lateral movement penalty, and the memory of difficult areas reduce the strain on the battery between charging cycles.

The specific energy consumption (Fig. 18) is 60.7 J/m for the proposed method and 74.1 J/m for the classical A* method, a reduction of 18.1%. Theta* + DWA and A* + DWA reach 66.1 J/m and 67.8 J/m, respectively; the error bars represent the variation between runs.

6. CONCLUSIONS

This paper analyzes the AMR platform from the perspective of the interdependence between the mechanical components, LiDAR, and trajectory. The modular frame, the four-point-guided lifting mechanism,

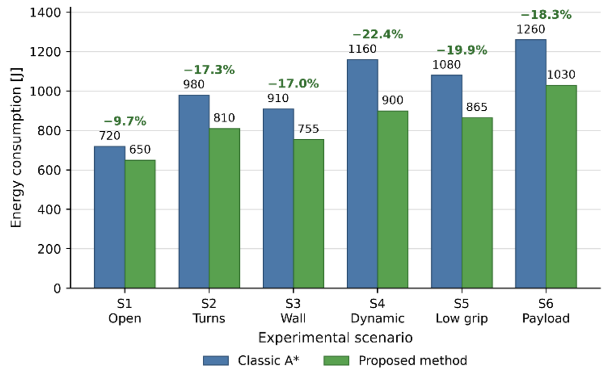

Fig. 16. Energy consumption in scenarios S1-S6: a comparison between the classical A* algorithm and the proposed method.

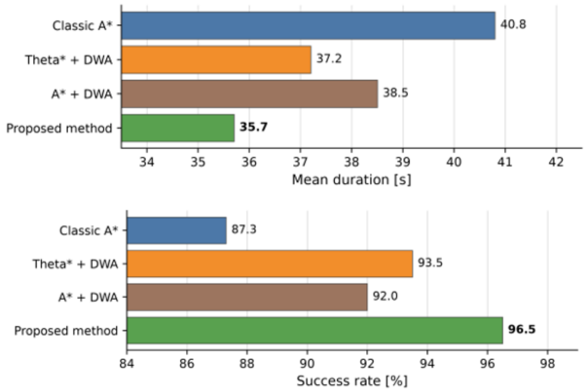

Fig. 17. Aggregate metrics for planning methods regarding duration and success rate.

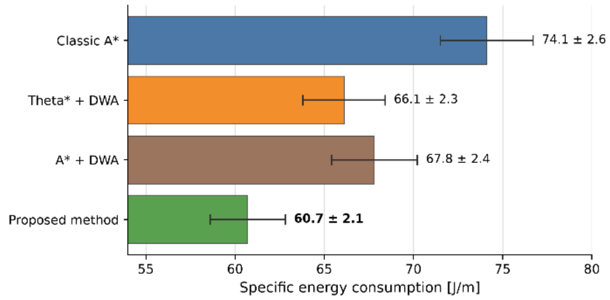

Fig. 18. Specific energy consumption for the compared planning methods.

and the base with four Mecanum wheels create a platform suitable for picking up shelves and maneuvering in confined spaces. Separating the vertical load from the lateral guidance limits the stress on the actuator, and mounting the LiDAR on the fixed frame maintains the sensor’s orientation during lifting.

For the measurement, the positioning conditions of the laser plane, the method for verifying the extrinsic transformation, and the main sources of error were defined. The calculation shows that the scanning frequency must be correlated with speed, since the platform can advance by tens of millimeters between two complete rotations. The tilt of the mount is critical: even a small angle can shift the scanning plane by tens of millimeters vertically at typical warehouse distances.

For trajectory control, the use of holonomic mobility is recommended on a selective basis. Longitudinal movement remains the primary mode along the lane, while lateral correction and diagonal movement are used for avoidance and docking. The T1–T4 protocol allows for the separation of LiDAR noise, vibration, kinematic error, and planner behavior. This separation reduces the risk of software adjustments being made to mask a mechanical cause.

The next step involves supplementing the protocol with measured data sets for various masses, surfaces, and speeds. The data must be reported along with the dispersion, not just as average values. This expansion may include automatic calibration of the laser frame, online estimation of slippage, and adaptation of the costmap margin to the current speed and direction. These developments retain the same basic idea: AMR performance is a property of the entire physical and informational chain.

REFERENCES

[1] SMD Components. Linear actuator LD3-24-20-K3 (product page). Available online: https://smd.ee/products/dc-linear-actuators/ld3-24-20-k3 (accessed on 31 August 2026).

[2] Moteck Electric Corp. LD3 Actuator—Product Data Sheet (PDF). Available online: https://www.moteck.com/proimages/1_products/LD3/LD3_Data_Sheet.pdf (accessed on 31 August 2026).

[3] Pololu. 30:1 Metal Gearmotor 37Dx68L mm 24V with 64 CPR Encoder (Helical Pinion), Product No. 4692. Available online: https://www.pololu.com/product/4692 (accessed on 31 August 2026).

[4] SLAMTEC. RPLIDAR A1M8—360 Degree Laser Scanner Development Kit (PDF). Available online: https://www.farnell.com/datasheets/3176118.pdf (accessed on 31 August 2026).

[5] Adafruit Industries. INA219 High Side DC Current Sensor—26V ±3.2A Max (product page). Available online: https://www.adafruit.com/product/904 (accessed on 31 August 2026).

[6] Lackner, M.; Hermann, J.; Kuhn, C.; Palm, D. Review of Autonomous Mobile Robots in Intralogistics: State-of-the-Art, Limitations and Research Gaps. Procedia CIRP 2024, 130, 930–935. doi:10.1016/j.procir.2024.10.187.

[7] Kubasakova, I.; Kubanova, J.; Benco, D.; Kadlecová, D. Implementation of Automated Guided Vehicles for the Automation of Selected Processes and Elimination of Collisions between Handling Equipment and People in a Warehouse. Sensors 2024, 24(3), 1029. doi:10.3390/s24031029.

[8] Macenski, S.; Jambrecic, I. SLAM Toolbox: SLAM for the Dynamic World. J. Open Source Softw. 2021, 6(61), 2783. doi:10.21105/joss.02783.

[9] Gatesichapakorn, S.; Takamatsu, J.; Ruchanurucks, M. ROS-Based Autonomous Mobile Robot Navigation Using 2D LiDAR and RGB-D Camera. ICA-SYMP 2019, pp. 151–154. doi:10.1109/ICAS-YMP.2019.8645984.

[10] Stefanini, E.; Ciancolini, E.; Settimi, A.; Pallottino, L. Safe and Robust Map Updating for Long-Term Operations in Dynamic Environments. Sensors 2023, 23(13), 6066. doi:10.3390/s23136066.

[11] Hart, P.E.; Nilsson, N.J.; Raphael, B. A Formal Basis for the Heuristic Determination of Minimum Cost Paths. IEEE Trans. Syst. Sci. Cybern. 1968, 4(2), 100–107. doi:10.1109/TSSC.1968.300136.

[12] Koenig, S.; Likhachev, M. D* Lite. In Proceedings of AAAI-02, Edmonton, AB, Canada, 28 July–1 August 2002; pp. 476–483.

[13] Nash, A.; Daniel, K.; Koenig, S.; Felner, A. Theta*: Any Angle Path Planning on Grids. In Proceedings of AAAI-07, Vancouver, BC, Canada, 22–26 July 2007; pp. 1177–1183.

[14] Kavraki, L.E.; Švestka, P.; Latombe, J.-C.; Overmars, M.H. Probabilistic Roadmaps for Path Planning in High-Dimensional Configuration Spaces. IEEE Trans. Robot. Autom. 1996, 12(4), 566–580. doi:10.1109/70.508439.

[15] LaValle, S.M. Rapidly-Exploring Random Trees: A New Tool for Path Planning. Tech. Rep. 98-11, Iowa State University, Ames, IA, USA, 1998.

[16] Xiang, D.; Lin, H.; Ouyang, J.; Huang, D. Combined Improved A* and Greedy Algorithm for Path Planning of Multi-Objective Mobile Robot. Sci. Rep. 2022, 12, 13273. doi:10.1038/s41598-022-17684-0.

[17] Lin, S.; Liu, A.; Wang, J.; Kong, X. A Review of Path Planning Approaches for Multiple Mobile Robots. Machines 2022, 10(9), 773. doi:10.3390/machines10090773.

[18] Maidana, R.; Granada, R.; Jurak, D.; Magnaguagno, M.; Meneguzzi, F.; Amory, A. Energy-Aware Path Planning for Autonomous Mobile Robot Navigation. In Proceedings ofFLAIRS-33, North Miami Beach, FL, USA, 17–20 May 2020; pp. 362–367.

[19] Xie, L.; Scheifele, C.; Xu, W.; Stol, K.A. Power Minimization and Energy-Reduction Autonomous Navigation of an Omnidirectional Mecanum Robot via the Dynamic Window Approach Local Trajectory Planning. Int. J. Adv. Robot. Syst. 2018, 15. https://doi.org/10.1177/1729881418754563.

[20] Mohammadpour, M.; Zeghmi, L.; Kelouwani, S.; Gaudreau, M.-A.; Amamou, A.; Graba, M. An Investigation into the Energy-Efficient Motion of Autonomous Wheeled Mobile Robots. Energies 2021, 14, 3517. https://doi.org/10.3390/en14123517.